THE ASTROPHYSICAL JOURNAL, 214:725–741, 1977 June 15

SEQUENTIAL FORMATION OF SUBGROUPS IN OB ASSOCIATIONS

BRUCE G. ELMEGREEN AND CHARLES J. LADA
Center for Astrophysics, Harvard College Observatory and Smithsonian Astrophysical Observatory
Received 1976 May 26; revised 1976 October 26

ABSTRACT

We reconsider the structure and formation of OB associations in view of recent radio and infrared observations of the adjacent molecular clouds. As a result of this reexamination, we propose that OB subgroups are formed in a step-by-step process which involves the propagation of ionization (I) and shock (S) fronts through a molecular cloud complex. OB stars formed at the edge of a molecular cloud drive these I-S fronts into the cloud. A layer of dense neutral material accumulates between the I and S fronts and eventually becomes gravitationally unstable. This process is analyzed in detail. Several arguments concerning the temperature and mass of this layer suggest that a new OB subgroup will form. After approximately one-half million years, these stars will emerge from and disrupt the star-forming layer. A new shock will be driven into the remaining molecular cloud and will initiate another cycle of star formation.

Several observed properties of OB associations are shown to follow from such a sequential star-forming mechanism. These include the spatial separation and systematic differences in age of OB subgroups in a given association, the regularity of subgroup masses, the alignment of subgroups along the galactic plane, and their physical expansion. Detailed observations of ionization fronts, masers, IR sources, and molecular clouds are also in agreement with this model. Finally, this mechanism provides a means of dissipating a molecular cloud and exposing less massive stars (e.g., T Tauri stars) which may have formed ahead of the shock as part of the original cloud collapsed and fragmented.

Subject headings: clusters: associations — interstellar: molecules — nebulae: general — stars: formation

I. INTRODUCTION

The Lyman continuum radiation from a cluster of OB stars will drive ionization (I) fronts into nearby neutral material. Near dense nebulae like M42 (Orion) or M17, an I front should be preceded by a shock (S) front as it moves into the adjacent molecular cloud. In this paper we investigate the gravitational stability of the high-density layer of neutral gas which accumulates between the I and S fronts in order to determine if star formation is likely to occur there. The results show that the shocked neutral layer will become gravitationally unstable after several million years for I-S fronts which propagate into molecular clouds of moderate density ($\gtrsim 10^3$ cm^{-3}).

The stars which may form as the layer collapses are likely to be more massive than those which form in the unshocked, remote parts of the same molecular cloud. This follows from the temperature dependence of the protostellar mass function (e.g., Silk 1976), and from the fact that the shocked layer will be slightly warmer than gas in other parts of the cloud because of the enhanced heat input in the immediate vicinity of the H II region (see § IV*b*[ii]). If, in fact, the stars which eventually form in the shocked layer are OB stars, then a new system of ionization-shock fronts will propagate into the remaining cloud after this second generation reaches the main sequence, and another cycle of OB star formation will be initiated. The formation of massive OB stars may therefore occur in sequential bursts during the lifetime of some large molecular clouds. For highly irregular clouds, the formation of massive stars may occur simultaneously at the sites of numerous I-S fronts, and a clear age sequence of OB stars may not develop. The birth of low-mass stars, however (e.g., T Tauri stars), may proceed independently and continuously throughout the cooler, more remote parts of the same molecular cloud. Most of these low-mass stars would probably remain obscured from view until they could be exposed during the passage of the I-S fronts (see § VI).

The observation that some nearby OB associations contain distinct, spatially separate subgroups of OB stars (Ambartsumian 1955) which lie along the galactic plane in a sequence of monotonically changing age (Blaauw 1964) led Blaauw to suggest that star formation did in fact occur in sequential bursts during the lifetimes of the corresponding primordial clouds. Recent millimeter and infrared observations of these regions suggest furthermore that the sequences of decreasing stellar ages may be extrapolated to cloudy regions where the most recent epochs of massive star formation are known to be occurring. In some cases, activity related to the formation of *massive* stars may actually be correlated with the positions of ionization fronts. Observations of NGC 7538, M17, and M8, for example, led to the suggestion that ionization fronts and their associated shock fronts may trigger massive star formation (Habing, Israel, and de Jong 1972; Lada *et al.* 1976*a*), and that these shocks may, at the same time dissipate the primordial cloud (Lada 1975; Lada *et al.* 1976*b*).

In § II, we review more observations which show why it is empirically quite plausible that I-S fronts may be a dynamic link between the OB subgroups which may form from any one complex of molecular clouds. In §§ III and IV, we present detailed calculations of the growth and gravitational stability of the dense layer which accumulates between plane-parallel I and S fronts. Time scales for the formation of OB stars and for the subsequent breakup of the shocked layer are shown in § V*a* to be in reasonable agreement with requirements from observations. Several interesting aspects of this particular mechanism of star formation are then discussed in § V*b*. These include the relative scaling of the times, distances, and cluster masses with the parameters which characterize the shock and the shock-driving OB subgroup, the tendency for the number of stars formed in a subgroup to converge to a constant value, and the alignment of subgroups along the cloud's magnetic field. Several comments are then made in § VI which pertain to star formation in general and how the proposed mechanism fits into an overall scheme. This is necessarily quite speculative, but it may indicate possible directions for future research. The results are summarized in § VIII.

II. OBSERVATIONS

The motivation for considering ionization-driven shock fronts as the mechanism responsible for sequential subgroup formation stems from recent observations of molecular and infrared emission from the dense neutral clouds which are adjacent to OB associations. In this section we review three well-studied cloud complexes which are associated with massive stars, visible emission nebulae, and therefore very recent star formation: M17, M42, and IC 1795(W3). Figure 1 shows a simplified schematic representation of the structure of these OB associations. In each of these cases, an expanding H II region, presumably caused by the OB-star ionization of cloud material, is located at the edge of a massive molecular cloud. Infrared sources, H_2O or OH masers, or compact continuum sources are observed in the cloud, indicating that star formation is under way. The important point, however, is that these active regions often occur near the interface between the H II region and the cloud at the expected location of an ionization-driven shock front.

Because of a favorable orientation along the line of sight, the relative positions of the various com-

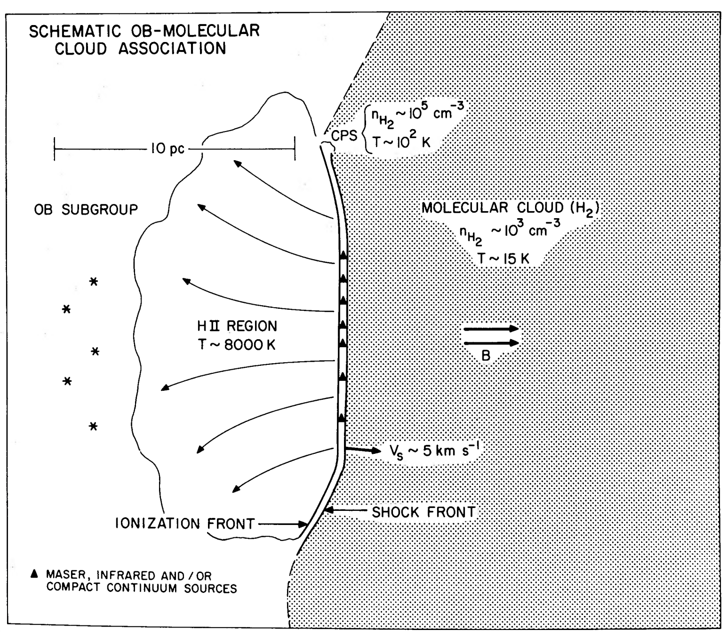

FIG. 1.—Schematic representation of the structure of an OB star–molecular cloud association. An OB subgroup (*) is positioned near the edge of a large molecular cloud (*shaded*). Ionizing radiation from the subgroup creates an H II region at the edge of the cloud, and drives an ionization-shock front into the cloud. After a certain time, the material that is swept up into a thin layer between the two fronts becomes gravitationally unstable and forms massive new stars. The figure shows the configuration at a time when the shocked layer has just formed stars. If the initial, uniform cloud density was 10^3 cm^{-3}, then the shock will have traveled some 10–15 pc in the 2 million years needed for the layer to become unstable. Although the newly formed stars are obscured at this time, H_2O and OH masers, infrared and/or compact continuum sources (▲) provide indirect evidence for their existence. In about a half-million years, the new OB stars will migrate out of and begin to destroy the shocked layer in which they formed. A new H II region will then be created and a new ionization-shock front will be driven into the remaining molecular cloud. The direction of the cloud magnetic field (B) is indicated for the ideal case. This direction is assumed to be parallel to the galactic plane in order to account for the observed alignment of OB subgroups (see text).

ponents of the M17 star-forming complex can be ascertained. East and north of the intense H II region (M17) are a group of visible OB stars which belong to the expanded Ser OB1 association (Sajn 1954). Embedded within the most intense part of the H II region is a compact, but obscured, cluster of OB stars recently discovered by infrared techniques (Beetz *et al.* 1976). Ionizing radiation from the most massive of these hidden stars is probably responsible for the excitation of the giant H II region. H_2CO and CO observations (Lada and Chaisson 1975; Lada 1975) have shown that the bright H II region is located at the edge of a massive molecular cloud which extends for more than 80 pc southwest of the visible nebula (Elmegreen and Lada 1976). Two dense ($\sim 10^4$ cm^{-3}) fragments of the neutral material are found at the edge of the cloud near the boundary of the H II region (Lada 1975). The northern fragment contains a far-infrared source and a weak radio continuum source while the southern contains two sites of H_2O maser emission and a 20 μm infrared source. These latter three objects are aligned along and very close to a strong ionization front which appears to be penetrating the southern fragment (Lada *et al.* 1976*a*). These data suggest that the site of star formation has moved with time from the position of the visible Ser OB1 stars to the position of the high-density fragments at the edge of the molecular cloud. The most intense region of ongoing star formation appears to be directly ahead of the strong ionization front which is now penetrating the southern fragment.

A similar configuration is present in the direction of Orion where a dense molecular cloud (Kutner *et al.* 1977), an expanding H II region (M42), and a sequence of four OB subgroups lie in an apparent evolutionary progression of young to old objects (cf. Fig. 4 of Blaauw 1964). Optical ionization fronts (Elliot and Meaburn 1974) are present near the densest part of the molecular ridge associated with the Kleinmann-Low infrared nebula, while another I front, observable in the radio continuum (Gull and Martin 1975), is preceded by, and parallel to, an array of maser sources in the OMC-1 cloud. The four Orion OB subgroups suggest that massive star formation has occurred in bursts which were separated in both space and time, as indicated by Blaauw (1964), while the current alignment of I fronts, masers, and infrared sources near M42 and OMC 1 supports our contention that ionization-driven shocks are somehow related to the gravitational collapse and formation of massive stars.

Of the three sources we consider here, the strongest evidence for the formation of massive stars at the interface between a molecular cloud and an H II region can be found near W3. The exciting source for the optical nebula (IC 1795) is probably the O8 star BD +61°411 located near the center of optical emission (Wynn-Williams 1971). Along the western boundary separating the H II region from an obscuring cloud are located a number of compact continuum, infrared, H_2O, and OH maser sources (Mezger and Wink 1975; Harris and Wynn-Williams 1976). The compact continuum and maser sources near IC 1795 seem to occupy the same relative positions to the H II molecular cloud interface as do maser and infrared sources in Orion and M17, but these regions of most recent star formation near IC 1795 seem more evolved than their counterparts in either Orion or M17 since the latter two regions have not yet produced detectable compact continuum sources.

The compact continuum sources in W3 probably represent recently formed OB stars which are currently ionizing their surrounding embryonic cloud envelopes. Indeed, recent infrared observations of Beetz *et al.* (1976) have uncovered a dozen OB stars near the centers of these compact continuum sources. This number is very similar to the number of OB stars typically found in the individual subgroups of the associations studied by Blaauw (1964; see Table 3). Interferometric observations of IC 1795 (Harris and Wynn-Williams 1976) suggest furthermore that the strongest continuum sources in W3 are ionization bounded on all sides and therefore are still embedded in and surrounded by the neutral material from which they formed. Consequently, the electron densities measured in these compact sources may provide a useful diagnostic for the conditions in the immediate region of star formation. These densities are generally greater than 5000 cm^{-3} and, in the case of W3(OH), the density is as high as 10^5 cm^{-3} (Wynn-Williams 1970). This is consistent with our expectations for the density of the shocked gas which precedes a typically strong ionization front (see eq. [20] below).

A sequence of stellar age groups is also present near W3. About 1° southeast of IC 1795 is the star cluster–H II region IC 1805, and slightly farther to the east of IC 1805 is the center of the Cas OB6 association. Sajn (1954) has suggested that these three objects, and perhaps IC 1848, are all part of the same complex and are physically related. We have recently made CO observations with the millimeter-wave telescope at McDonald Observatory which show that the molecular cloud which partially envelops W3 extends south and southeast and also forms the border of the IC 1805 H II region. This suggests that the two objects IC 1795 and IC 1805 were formed from the same molecular cloud complex. If these two sources are at the same distance from the Earth, then their separation is roughly 50 pc, comparable to, but slightly larger than, the separations of OB subgroups in the associations listed by Blaauw (1964). The star cluster at the center of IC 1805 is presumably more evolved than the embedded cluster in IC 1795 (Mezger and Wink 1975). As in many other associations, direction of evolution is parallel to the galactic plane.

Similar evolutionary sequences (i.e., OB association–ionization front–protostars–molecular cloud) can be recognized in observations of other associations such as Cep OB3 (cf. Fig. 4 of Blaauw 1964) and Cep OB4 (McConnell 1968; Churchwell and Felli 1970), W58 (Israel 1976), and M8 (Lada *et al.* 1976*b*). This suggests that the formation process for OB subgroups may be similar for all OB associations, and that it may be physically related to the ionization-shock front systems. The observed structure of OB associations also seems to require that OB stars are first formed at the edge of a cloud and not in its center (Blaauw 1962) and that subsequent star formation proceeds inward with time. If ionization-shock front systems are responsible for star formation in OB associations, then the observed sequential progression of subgroup age could be explained by a chain reaction in which the formation of the youngest subgroup is triggered by the ionization fronts driven into the cloud by the next older subgroup. Apparently, this sequence can be extrapolated to the most recent episodes of star formation in the molecular clouds which are adjacent to associations.

III. MODEL

The observed juxtaposition of (1) young OB stars, (2) I fronts, infrared sources, masers, and/or compact continuum sources, and (3) dense molecular clouds is interpreted to be an indication of a sequence in time during which some star-forming part of an I-S front moves through a dense molecular cloud. For the purposes of the present calculation, we assume that the primordial molecular cloud has a linear dimension at least as large as the typical separation between subgroups—i.e., some 10–20 pc—and that it has a density comparable to that of observed molecular clouds, although this density will remain a free parameter. We also assume that the cloud is relatively stable, in the sense that it does not completely collapse in a time less than the observed interval between the formation of adjacent subgroups, i.e., 2–3 million years. In the case of Orion, for example, OB star formation has been occurring in the same molecular cloud complex for the last 10 million years, so this assumed stability is probably not unreasonable. This is also true for other large molecular clouds as pointed out by Strom *et al.* (1975*a*).

We then consider the dynamical influence of an *extended* OB subgroup which happens to be adjacent to this hypothetical molecular cloud. The Lyman continuum (LC) radiation from this OB subgroup will dissociate, ionize, and heat the neutral and molecular hydrogen in the molecular cloud via the propagation of ionization (I) and dissociation fronts. A short time after the OB subgroup first turns on, given approximately by $(n\alpha)^{-1} \approx 100$ years, where $n \approx 10^3$ is the H density in the cloud and $\alpha = 3.1 \times 10^{-13}\ \mathrm{cm^3\ s^{-1}}$ is the recombination coefficient of hydrogen to all but the ground state at 8000 K, the LC flux at the I front will diminish due to dilution and to absorption in the intervening H II region. A shock front will then move out ahead of the I front, compressing the neutral material before it becomes ionized. The various stages in the propagation of I-S fronts are summarized by Kahn (1954), and are applied to astrophysical situations similar to that discussed here by Oort and Spitzer (1955), Pottasch (1958), Lasker (1967), and Elmergreen (1976).

We are primarily concerned here with the neutral layer which separates the I and S fronts. Since the radiative cooling of this layer will be relatively rapid (see Aannestad 1973), the temperature of the shocked gas will be low ($\lesssim 100$ K) and the density will be very high ($\sim 10^5\ \mathrm{cm^{-3}}$ as shown below). Furthermore, the molecular hydrogen which enters and becomes heated by the shock front will cool before it collisionally dissociates (Mendis 1968), so H_2 will still be present. We shall hereafter refer to this region between the I and S fronts as a cooled, postshock (CPS) layer. Its growth and gravitational stability will be studied in what follows. Although we shall use a plane-parallel geometry due to the extended nature of the shock-driving OB subgroup, the results will be qualitatively the same for a spherical (but thin) CPS layer which propagates away from a point source of LC radiation.

The absorption of Lyman continuum radiation by dust in the H II region is discussed briefly in § IV*b*(i). Although the dynamics of the propagation of the I-S front into the molecular cloud will be slightly influenced (and made more complex) by interstellar dust, the important star-forming properties of I-S fronts are not changed. Of course, interstellar dust will be an important factor in the thermal balance of the shocked gas and protostars, but this will be implicit in our use of a relatively high gas temperature in the shocked region of 100 K. This is suggested by the infrared (dust) temperatures of the region ahead of an I front in Orion (presumably the shocked gas) observed by Becklin *et al.* 1976 (cf. §IV*b*[ii]).

IV. GRAVITATIONAL INSTABILITIES IN THE VICINITY OF AN H I–H II INTERFACE

a) *The Development of the CPS Layer*

We first derive the velocity of a planar shock relative to the ambient cloud. The position of the shock is then determined as a function of time, and the column density, space density, and thickness of the CPS layer are written as a function of the shock position. These latter quantities will be used in § IV*b* to determine when the CPS layer becomes gravitationally unstable and to estimate the protostellar masses.

The shock velocity depends on the thermal pressure in the H II region, P_{II}, on the rocket-like pressure, or kinetic pressure, at the I front (which is caused by the ejection of newly ionized hydrogen into the H II region), and on the mass density of the molecular cloud, ρ_0. Since the post-I-front gas will rapidly cool to the temperature of the H II region, the equation of state for ionized gas sufficiently far from the I front will be isothermal, as it is behind the S front, and the *steady state* shock velocity, v_s, will equal $(\xi P_{\mathrm{II}}/\rho_0)^{1/2}$, where ξ varies from 1 for weak D-type fronts to 2 for D-critical fronts (Spitzer 1968*b*). In the first case the flow behind the I front will be subsonic and the kinetic pressure will be insignificant compared to P_{II}, while in the second case the ionized flow will be sonic and the kinetic pressure will equal the thermal pressure.

The relative importance of the thermal and kinetic pressures is determined by the flux of LC radiation at the I front and by the hydrodynamics of the flow in the H II region, which are beyond the scope of the present paper. We may estimate that $\xi \approx 2$, however, from observations of Orion (Balick, Gammon, and Hjellming 1974), M8 (Lada *et al.* 1976*b*) and other dense nebulae (Meaburn 1975) since these always show large outflows of ionized hydrogen at near sonic velocities, suggesting that a kinetic pressure will be significant. We therefore assume for simplicity that $\xi = 2$, at least for the initial stages of shock propagation. We have also considered the hypothetical situation where ξ jumps abruptly from 2 to 1 after the shock has traveled for some time. This simulates a change which may occur as the nebula becomes large and rarefied: the boundary conditions on the flow may change due to obstacles (e.g., other clouds) at moderate distances from the molecular cloud or the LC flux of the source may change. In any case, the later stages in the expansion of the H II region may be similar to the quasi-equilibrium expansion of a Strömgren sphere, for which $\xi \approx 1$. This change from $\xi = 2$ to $\xi = 1$ at a late stage in the development of the shock will have a slight influence on the formation time of protostars in the CPS layer, so we shall discuss this briefly in § IV*b*(i).

It should be emphasized that the above expression for v_s is valid for constant v_s, i.e., for a steady state, but in the present problem $P_{\rm II}$, and therefore v_s, will decrease as the shock advances into the cloud and, if the momentum of the CPS layer is significant, v_s will be slightly larger than $(\xi P_{\rm II}/\rho_0)^{1/2}$. We therefore determine v_s in two steps. First, the steady state value of the proton density in the H II region, $n_{\rm II}$, is derived for a given value of the distance r between the LC source and the I front. The time rate of change of $n_{\rm II}$ due to the increase of r at the shock velocity is shown to be small compared to the rate at which the density can sonically adjust, so we approximate the instantaneous value of $n_{\rm II}$ by its steady state value. Thus $P_{\rm II}$, which depends on $n_{\rm II}$, may be written simply as a function of r. The second step then determines v_s by equating the total pressure on the I front, $\xi P_{\rm II}$, to the time rate of change of the momentum per unit area of the CPS layer. This will apply to the plane-parallel case considered here since the area of the shock is invariant, but for a spherical shock around a point LC source the total force and total momentum of the CPS layer must be considered.

The boundary conditions at the I front and far from the molecular cloud determine the run of $n_{\rm II}$ with distance r. In the present model, an extended LC source (the OB subgroup) is relatively near to an extended molecular cloud, so the LC photon flux and the flow of ionized hydrogen in the H II region will be approximately plane-parallel and $n_{\rm II}$ will be relatively uniform throughout the small distance r. The velocity of flow away from the I front, $v_{\rm ex}$, will also be approximately uniform in this region, although it will vary for larger distances from the I front. The proton flux at the I front, $n_{\rm II}v_{\rm ex}$, will then equal the stellar LC flux, F_*, diminished by the number of absorptions in a column of unit area and length r. In the absence of dust (see § IV*b*[i]), this absorption rate will equal the recombination rate in the same volume, so we have

$$n_{\rm II}v_{\rm ex} = F_* - n_{\rm II}^2\alpha r\,. \qquad (1)$$

For the assumed plane parallel geometry, F_* will be independent of r. The solution for $n_{\rm II}$ is

$$n_{\rm II} \approx \left(\frac{F_*}{\alpha r}\right)^{1/2}\left(1 - \frac{v_{\rm ex}}{2n_{\rm II}\alpha r}\right) \approx n_0\left(\frac{r_0}{r}\right)^{1/2}, \qquad (2)$$

where n_0 is the number density of hydrogen in the molecular cloud and $r_0 = F_*/(\alpha n_0^2)$ is the thickness of a hypothetical layer of ionized hydrogen at a density n_0 which can be maintained by the stellar flux F_*. The second term in parentheses in equation (2) is the ratio of the recombination time of hydrogen at the density $n_{\rm II}$ (to all but the ground state) to the time for the flow to travel the distance r. This ratio will be very small ($<1\%$) for typical values of $n_{\rm II}$ and r.

Thus $n_{\rm II}$ must decrease with time at the relative rate of $d\ln n_{\rm II}/dt = -\frac{1}{2}v_s/r$ as the shock advances into the molecular cloud. The rate at which $n_{\rm II}$ is able to change, however, is approximately equal to the isothermal sound crossing rate in the H II region, or c/r, where $c = (P_{\rm II}/\rho_{\rm II})^{1/2} = v_s[3\rho_0/(8\rho_{\rm II})]^{1/2} \approx v_s(3/8)^{1/2}(r/r_0)^{1/4}$ using equations (2) and (6) below with $\xi = 2$. Thus $c/r \gg \frac{1}{2}v_s/r$ if $r/r_0 \gg 0.4$. Since the shock begins approximately when $r = r_0$, this inequality is always satisfied and the density can always adjust so that it approximates that given by equation (2). The thermal pressure in the H II region is therefore

$$P_{\rm II} = 2.1n_0\left(\frac{r_0}{r}\right)^{1/2}kT_{\rm II} \qquad (3)$$

for an H II temperature $T_{\rm II}$ and for 10% helium by number.

The shock velocity in the nonsteady case may now be determined by equating the total pressure which acts on the I front ($\xi P_{\rm II}$) to the time rate of change of the momentum per unit area of the CPS layer. The mass per unit area of the CPS gas changes at a rate equal to the difference between the mass flux at the S front and the mass flux at the I front. As shown below (eq. [11]), the first will be much larger than the second when $r \gg r_0$, so we may use $\rho_0 r$ as an approximation for the mass column density of the CPS gas, which will be valid in the limit of large r. The velocity of the center of mass of the CPS layer, used to determine the CPS momentum, is so close to v_s for strong isothermal shocks that we may effectively set it equal to v_s. Then the momentum per unit area of the CPS layer will equal $\rho_0 r v_s$ for $r \gg r_0$ and

$$\xi P_{\rm II} = \frac{d}{dt}(\rho_0 r v_s) = \rho_0 v_s^2 + \rho_0 r\frac{d}{dt}v_s \qquad (4)$$

since $v_s = dr/dt$. However, $P_{\rm II}$ varies as a power of r, so v_s^2 will vary with the same power of r (from eq. [4], ignoring slow changes in ξ), and, using equation (3), we obtain

$$\frac{d}{dt}v_s = -\frac{v_s^2}{4r}\,. \qquad (5)$$

Combining equations (3), (4), and (5), we conclude that

$$v_s = (\tfrac{4}{3}\xi P_{\mathrm{II}}/\rho_0)^{1/2} . \tag{6}$$

The shock velocity will actually vary between $(\xi P_{\mathrm{II}}/\rho_0)^{1/2}$ and that given by equation (6) as r/r_0 increases and the momentum of the CPS layer approaches $\rho_0 r v_s$, but this variation will not significantly influence the results so we simply use equation (6) for all r. (This has been verified by a numerical integration.)

Thus v_s may be evaluated from equations (3) and (6). It is convenient to set $F_* \equiv 1.0 \times 10^{11}\, N_{\mathrm{O}}$ photons $\mathrm{cm^{-2}\, s^{-1}}$, where N_{O} is the effective number of main-sequence O stars per 10 pc^2 in the OB subgroup whose radiation drives the shock. The LC luminosity of a typical main-sequence O star has been taken to be 1×10^{49} photons $\mathrm{s^{-1}}$ from Cruz-Gonzales *et al.* (1974), and an O star column density of 10 per 100 pc^2 has been estimated from the compilation of Blaauw (1964). We expect therefore that N_{O} will be of order unity. The results will be fairly insensitive to N_{O} in any case. We also define $n_3 \equiv 10^{-3}\, n_0 = 10^{-3}\, \rho_0/1.4 m_{\mathrm{H}}$ for hydrogen atomic weight m_{H}, so that n_3 is also of order unity or larger for dense molecular clouds. Finally, we take $\xi = 2$ for the present discussion, $T_{\mathrm{II}} = 8000$ K, and the corresponding value of $\alpha = 3.1 \times 10^{-13}\ \mathrm{cm^3\, s^{-1}}$ so that, for r in parsecs,

$$v_s(r) = 9.4 r^{-1/4} N_{\mathrm{O}}^{1/4} n_3^{-1/2}\ \mathrm{km\ s^{-1}} . \tag{7}$$

Since $v_s = dr/dt$, equation (7) may be integrated to obtain the shock position as a function of the time t_6 in millions of years:

$$r(t_6) = (r_0^{5/4} + 12.1 N_{\mathrm{O}}^{1/4} n_3^{-1/2} t_6)^{4/5}\ \mathrm{pc} , \tag{8}$$

where

$$r_0 = 0.10 N_{\mathrm{O}} n_3^{-2}\ \mathrm{pc} \tag{9}$$

from equation (2). For r much larger than r_0 or for times much greater than 8×10^4 years since the formation of the shock-driving OB subgroup, we may approximate this as

$$r \approx 7.3 N_{\mathrm{O}}^{1/5} n_3^{-2/5} t_6^{4/5}\ \mathrm{pc} . \tag{10}$$

The column density N of hydrogen (protons) in the CPS layer is the integral over time of the total rate of proton accumulation, $n_0 v_s - n_{\mathrm{II}} v_{\mathrm{ex}}$. For D-critical I fronts we may set v_{ex} equal to the isothermal sound speed in the H II region; it then follows from equations (2), (7), and (8) that

$$N = 3.09 \times 10^{21} r n_3 \left[1 - 0.18\frac{r_0}{r} - 0.82\left(\frac{r_0}{r}\right)^{1/4}\right] \mathrm{cm^{-2}} , \tag{11}$$

where again r is in parsecs. The last two terms in the brackets, when added to (r_0/r), correspond to the CPS material which has become ionized. For $r/r_0 > 8.3$, less than half the hydrogen which enters the shock will have gone through the I front, so the approximation used to derive v_s is beginning to be reasonable. For weak-D I fronts at the same r, the CPS layer will have a larger column density than that given by equation (11) since the proton flux at the I front will be less. This is discussed in § IV*b*(i).

Since the shock decelerates, the density in the CPS layer will not be uniform but will increase toward the front of the layer as if there were an effective gravity with acceleration $-\dot{v}_s$ in the direction of propagation of the shock. If the layer is not strongly self-gravitating, the scale height will be $c^2/(-\dot{v}_s)$ for isothermal sound speed $c = (kT/\mu_c)^{1/2}$ in the CPS layer, and the density at the leading edge of the layer will be $(8/3)P_{\mathrm{II}}/c^2$ (for $\xi = 2$). Here T is the temperature in the layer which we set equal to 100 K times a constant T_2, which is of order unity, and $\mu_c = 2.36\, m_{\mathrm{H}}$ for molecular hydrogen with a 10% helium-to-proton ratio. It may be easily shown that the sound crossing time in the CPS layer is much smaller than the time scale for changes in P_{II}, so the CPS density distribution will be close to this hydrostatic solution except for possible changes due to turbulence in the Rayleigh-Taylor instability mentioned below. Using equations (3), (5), (7), and (9), we see that the hydrogen density will vary with position z in the CPS layer as

$$n_c(z) = 2.4 \times 10^5 r^{-1/2} N_{\mathrm{O}}^{1/2} T_2^{-1} \times \exp\{-60.4 z r^{-3/2} N_{\mathrm{O}}^{1/2} n_3^{-1} T_2^{-1}\}\ \mathrm{cm^{-3}} , \tag{12}$$

where z (in parsecs) equals zero at the front of the CPS layer (close to the shock) and increases to $z = L$ at the I front. This CPS thickness L is determined by the total column density of the CPS gas, since the integral of n_{CPS} over z from $z = 0$ to $z = L$ must equal N in equation (11). It follows that the thickness of the CPS layer is given by

$$L \approx 4.8 \times 10^{-3} r^{3/2} N_{\mathrm{O}}^{-1/2} n_3 T_2\ \mathrm{pc} \tag{13}$$

for $r \gg r_0$ in equation (11), when the layer is not strongly self-gravitating.

Another consequence of the deceleration of the CPS layer is that it will be Rayleigh-Taylor unstable with a growth rate equal to $(-k\dot{v}_s)^{1/2}$ for wavenumber k. For k greater than or equal to $2\pi/L$, the growth time is much shorter than any of the temporal scales for the shock propagation, and the instability will be present. Unstable blobs will not be ejected from the front of the layer, however, because if they were they would decelerate even faster than the rest of the shock as they accumulate material. The most likely result is that the CPS layer will become turbulent. We may estimate the turbulent velocity by using the "free-fall" velocity of a blob which accelerates over a length equal to $L/2$. This velocity is $(-\dot{v}_s L)^{1/2}$, so we have that

$$v_{\mathrm{turb}} \approx 0.3 T_2^{1/2}\ \mathrm{km\ s^{-1}} . \tag{14}$$

Note that this is independent of all the parameters which characterize the shock (N_{O}, n_3, etc.), and it depends only on the temperature in the CPS layer. This value of the turbulent velocity is equal to $(\ln 4/3)^{1/2}$, or about one-half, times the sound velocity of CPS gas. Such turbulence may be accounted for in the derivation of the gravitational instability by using a slightly larger value of the temperature in the CPS layer to correspond to a larger rms velocity (cf. § IV*b*[ii]), but there is enough uncertainty in this temperature anyway that such a change is unwarranted.

Evidently the CPS layer will be very thin and dense. After a sufficient amount of material has accumulated, its self-gravitation will become important. This will cause the density inside the layer to increase above the value given by equation (12), and the thickness of the layer will decrease accordingly. These changes are discussed in detail in the Appendix, as is the criterion for the onset of gravitational instability of the CPS layer. We use the results in what follows.

b) *The Onset of Gravitational Instability in the CPS Layer*

i) *The Point of Instability for D-critical I Fronts* ($\xi = 2$)

It is shown in the Appendix that the pressure which confines the CPS layer will stabilize it against gravitational collapse until the mass column density of the CPS gas, σ, reaches a critical value, σ_m, given by equation (A17), in the case where $\gamma \equiv (1 + \dot{v}_s r/v_s^2)^{-1} = 4/3$; that is, where v_s is proportional to $r^{-1/4}$. Using equations (3) and (11) which assume that the dust in the H II region does not significantly absorb the LC radiation, and using the fact that σ equals $1.4m_H$ times the hydrogen (proton) column density given in equation (11), it follows that the CPS layer will begin to gravitationally collapse when the shock has traveled a distance r_I, given by the solution to the equation

$$r_I^{5/4}\left[1 - 0.18\frac{r_0}{r_I} - 0.82\left(\frac{r_0}{r_I}\right)^{1/4}\right] = 28.1\, N_O^{1/4} n_3^{-1}\,, \quad (15)$$

which, for $N_O = n_3 = 1$ in equation (9), is $r_I = 17.7$ pc. For $N_O n_3^{-2} \ll 1$ in equation (9),

$$r_I \approx 14.4 N_O^{1/5} n_3^{-4/5}\ \text{pc} \quad (r_I \gg r_0)\,. \quad (16)$$

The time at which this instability occurs is

$$t_I \approx \frac{r_I^{5/4} - r_0^{5/4}}{12.1 N_O^{1/4} n_3^{-1/2}}\ \text{million years} \quad (17)$$

from equation (8), which equals 3.0 million years when $N_O = n_3 = 1$. It follows that when $N_O n_3^{-2} \ll 1$,

$$t_I \approx 2.3 n_3^{-1/2}\ \text{million years} \quad (r_I \gg r_0)\,. \quad (18)$$

We note that, in the case of Orion, $N_O n_3^{-2}$ is probably less than 10^{-2} since $n_3 > 10$ (i.e., the hydrogen [proton] density in the Orion molecular cloud is greater than 10^4 cm^{-3} [Gottlieb *et al.* 1975]) and $N_O \approx 1$ from Blaauw (1964); thus equations (16) and (18) are applicable for the current epoch of star formation in Orion (if dust can be ignored). Dust in the H II region may absorb some of the LC radiation and will thereby lower the electron density (n_{II}) and the pressure which drives the shock. The result is that the position of the shock at the time of instability (r_I) will be less than that given by equation (15) or (16), but the unstable time (t_I) is virtually unchanged (cf. § V*b*). We find from a numerical calculation with $N_O = n_3 = 1$ and $\xi = 2$ that (with dust) $r_I = 11.6$ pc and $t_I = 2.6$ million years. (These parameters are not solutions to the instability criterion given by eq. [A17], which uses a constant γ equal to 4/3, but they use the instantaneous value of $\gamma = [1 + \dot{v}_s r/v_s^2]^{-1}$ from the numerical solution to derive an instantaneous instability criterion.)

If the I-front is always weak D ($\xi = 1$) or if it changes from D-critical ($\xi = 2$) to weak D during the course of its propagation into the molecular cloud, then the unstable distance and time will also be less than that given by equation (16) and (18). The results indicate that t_I will decrease by about 20% and r_I will decrease by a factor of 23% to 33%, depending on the point at which the I front changes from D-critical to weak D. This depends on the geometry of the cloud and on the details of the flow in the H II region which are not considered here.

ii) *The Development of Protostars*

Evidently, the CPS layer will become unstable to gravitational collapse after a time of some 2 to 3 million years for a hydrogen density in the molecular cloud of 10^3 cm^{-3}, decreasing for larger densities approximately as $n_3^{-1/2}$. The shock will have traveled a distance of 10–20 pc in this time, scaling roughly as $N_O^{1/5} n_3^{-4/5}$ for this plane-parallel model. Of course, the exact times and distances will depend on the geometry and homogeneity of the cloud, on the details of the flow in the H II region, and on the contribution to the absorption of LC radiation by dust.

In general, shorter unstable distances and times are possible if the I front becomes weak D before the CPS layer collapses or if dust absorption is included. We therefore assume for the present discussion that reasonable values for the unstable distances and times are given by

$$\bar{r}_I = 13 N_O^{1/5} n_3^{-4/5}\ \text{pc}\,, \quad (19a)$$

and

$$\bar{t}_I = 2.6 n_3^{-1/2}\ \text{million years}\,, \quad (19b)$$

in comparison to equations (15) and (17). Values similar to this may be obtained from either a numerical solution with dust absorption for $N_O = 1$ and $n_3 =$ 1–10, or from the dust-free case with a change in ξ from 2 to 1 at $r_\xi/r_{\xi I} = 0.5$, or for $r_0 \ll r_I$ (cf. eqs. [16] and [18]). Any combination of these three conditions will lower $\bar{r}_I$ and $\bar{t}_I$ somewhat more. On the other hand, the criterion for gravitational instability in the CPS layer (eq. [A17]), used to obtain $\bar{r}_I$ and $\bar{t}_I$, only determines when the layer will become unstable to very large perturbations ($\nu = 0$); protostars will actually form at a slightly later time, when smaller lengths become unstable. In any case, we may use equations (19a) and (19b) and $\xi \approx 1$ at $r = r_{\rm I}$ to illustrate the sequence of events which occurs after the instability begins.

For typical values of $N_{\rm O}$ and n_3, the density in the CPS layer will be very large at the onset of gravitational instability, and the ensuing collapse will be relatively rapid. Using the hydrostatic distribution of density which was derived in the Appendix, we obtain a maximum density in the layer of

$$\rho(0) = 3.8\, P_{\rm II}/c^2$$
$$= 2.1 \times 10^{-19} N_{\rm O}^{2/5} n_3^{2/5} T_2^{-1}\ \mathrm{g\ cm^{-3}}\ , \quad (20)$$

from equation (A8) with $P_1 = P_{\rm II}$ evaluated at $r = \bar{r}_{\rm I}$, using a temperature of 100 K (i.e., $T_2 = 1$) and a mean molecular weight of $2.36 m_{\rm H}$. This corresponds to a hydrogen (proton) density of 1.0×10^5 cm^{-3}. The growth time of a Jeans instability given by $[4\pi G\rho(0)]^{-1/2}$ is a good measure of the protostellar collapse time, and is

$$\tau_{\rm J} = 7.5 \times 10^4 N_{\rm O}^{-1/5} n_3^{-1/5} T_2^{1/2}\ \mathrm{years}\ . \quad (21)$$

After this relatively short collapse time, the protostars will become sufficiently compact to be independent of the pressure forces exerted by the surrounding gas and they will drift into the cloud at a constant velocity, approximately equal to the shock velocity at $\bar{r}_{\rm I}$ given by equation (6) with $\xi = 1$:

$$v_s(\bar{r}_{\rm I}) = 3.5 N_{\rm O}^{1/5} n_3^{-3/10}\ \mathrm{km\ s^{-1}}\ . \quad (22)$$

(It is interesting that observations indicate that the Trapezium cluster is approaching the nearby Orion molecular cloud at about this velocity, i.e., 3 km s^{-1} [Zuckerman 1973]). The shock continues to slow down according to equation (7), however, so the relative velocity between the shock and the stars increases at a rate equal to $-\dot{v}_s$. After a time, $\tau_{\rm em}$, approximately equal to $(-L/\dot{v}_s)^{1/2}$ for CPS layer thickness L the stars will emerge from the front of the layer. Using equations (5) and (6) with $\xi = 1$ and a layer thickness L from equation (A22), we obtain

$$\tau_{\rm em} = 5.6 \times 10^5 N_{\rm O}^{-1/5} n_3^{-1/5} T_2^{1/2}\ \mathrm{years}\ . \quad (23)$$

Comparing equations (21) and (23), we see that the free-fall time is much less than the emergence time, so the initial stages in the collapse of a protostar will be relatively complete before the protostar emerges from the front of the layer. Of course, when the protostar becomes optically thick to cooling radiation, it will contract to the main sequence on a Kelvin-Helmholtz time scale, which is less than 4×10^4 years for O stars (Herbig 1960). Thus an O star may emerge on the main sequence for typical $N_{\rm O}$ and n_3. This is assumed in § V*a*.

The total mass of the CPS layer scales with the area of the star-forming part of the shock. Using an estimated dimension of 3 pc by 3 pc for the region of most intense star formation (see the discussion in § V*b* [iii] on the magnetic alignment of subgroups), this becomes

$$M_{\rm CPS} = 3100 N_{\rm O}^{1/5} n_3^{1/5}\ M_\odot\ . \quad (24)$$

The fraction of this CPS mass which actually forms stars is uncertain, as are the dimensions used to calculate it. It is probably significant that this CPS mass is several times the average mass of a subgroup ($10^3\ M_\odot$ from Blaauw 1964), so there is adequate protostellar material available even if the efficiency is low.

The protostellar masses depend on the details of the fragmentation of the CPS layer and on the final stages of gravitational collapse. There are several reasons why star formation between I and S fronts may lead to more massive stars than in the case of a fragmenting cloud. One follows from the fact that the temperature in the CPS gas will be higher than that far ahead of the shock due to the heat input by the warm, radiating dust in the nearby H II region. Observations of an edge-on I-S front in Orion support this (Becklin *et al.* 1976): dust temperatures are observed to be in the range of 60–300 K. A simple calculation shows that gas at a density of 10^5 cm^{-3} can in fact be heated to about 100 K by the warmer dust component of Becklin *et al.* The mass of a fragment which has just become optically thick (and therefore stops further fragmentation) depends sensitively on its temperature: for graphite and ice-mantel grains, this threshold mass scales roughly with T^3 while for other grain compositions the power of T is even larger (Silk 1976). Thus protostellar masses will be much larger in the warm CPS layer than they will be in the distant, cooler parts of the molecular cloud. For the same reason, the mild Rayleigh-Taylor instability in the CPS layer may increase the protostellar mass by making the gas subsonically turbulent, thereby increasing the rms velocity of the CPS gas and simulating a larger temperature.

Another reason we might expect larger masses in the CPS gas may involve the coalescence of the optically thick fragments. If the increase in T alone is not sufficient to make 20 $M_\odot$ stars, for example, then such stars may be the result of collisions between the critical mass fragments. These collisions may be more frequent in a plane-parallel geometry than in a sphere. The extent to which this can influence the mass function is unknown.

A possible indication of the protostellar mass may be the mass, $M_{\rm cyl}$, in a cylinder through the CPS layer, the base of which has a diameter equal to the layer thickness. Using $L = z_1 + z_2$ for this thickness from equation (A22), we find that

$$M_{\rm cyl} = \tfrac{1}{4}\pi(z_1 + z_2)^2 \sigma_m = 6.7 N_{\rm O}^{-1/5} n_3^{-1/5} T_2^{2} M_\odot\ . \quad (25)$$

Initially the transverse scale of the instability will be much larger than $z_1 + z_2$ (since $\nu < 1$), so we may expect that the final mass of a protostar may be more like M_{cyl}/ν^2. This could be quite large, depending on the manner in which the CPS layer collapses.

Our conclusion cannot be definite until a proper analysis of the mass function is made. There is reason to believe, however, that CPS star formation may lead to more massive stars than will the fragmentation of a cool molecular cloud. Thus we postulate that OB stars (and possibly less massive stars as well) will be made as the CPS layer collapses. This will then complete the cycle of periodic OB subgroup formation.

V. DISCUSSION

The propagation of the ionization-shock front which is driven into a molecular cloud by the LC radiation of a nearby OB subgroup has been followed until the cool layer of gas which accumulates between the I and S fronts became gravitationally unstable. The density of this self-gravitating layer was then shown to be so high that the collapse of the protostars will be relatively rapid, and a new star cluster will almost immediately form. A rough estimate of the protostellar masses indicated that this new cluster may also contain OB stars and that the total mass of the unstable gas was sufficient to form a new OB subgroup. We expect, therefore, that a new I-S front, similar to the first, will be driven by the LC radiation of the new OB cluster, and that this will advance further into the cloud, causing the entire sequence of star formation to be repeated provided sufficient cloudy material remains. The same LC radiation may also be expected to cause the breakup of the remainder of the CPS layer, thus exposing the new stars. We discuss this breakup here in § V*a*.

The observed sequence of OB subgroups may thus be readily explained. The spatial separation and age difference between subgroups would then be caused by the delay in the propagation of the shock before the CPS layer becomes gravitationally unstable. Several other aspects of OB associations also follow from this analysis. These concern the degree of regularity of subgroup separations, ages, and total masses, their observed (approximate) alignment along the galactic plane, and their expansion. We discuss these topics in § V*b*.

a) The Breakup of the CPS Layer

The results of § IV*b*(ii) indicate that the stars which form in the CPS layer will drift out of the front of the layer in about one-half million years as the shock continues to slow down. Their LC radiation will therefore drive a new I-S front into the ambient molecular cloud and the new, high-pressure H II region which forms between the molecular cloud and the old CPS layer will drive a shock back into the old CPS layer. The pressure P which drives this shock back is of order 2.1 n_0kT_{II} because the H II gas will not expand much until the CPS layer breaks apart and the H II density will still be that of the primordial cloud; the preshock density will be the density in the CPS layer, which is approximately the mass column density in the layer σ_m divided by the thickness L of the layer. The time scale for the propagation of the shock τ_D is thus L divided by the shock velocity, or approximately $(L\sigma_m/P)^{1/2}$. Using equations (2), (3), and (23), we obtain

$$\tau_D = \tau_{em}\left(\frac{1}{3}\right)^{1/2}\left(\frac{r_0}{r_I}\right)^{1/4} = 0.17\tau_{em}N_0^{1/5}n_3^{-3/10} . \tag{26}$$

The newly shocked CPS layer will begin to disperse after the time τ_D as a result of a Rayleigh-Taylor instability. The low-density fluid is the new H II region, and this pushes on a high-density fluid, the twice-shocked CPS gas, causing it to accelerate. The rate of growth of the instability is the square root of the product of the unstable wavenumber and the acceleration. Since the acceleration is of order P/σ_m and the layer thickness is roughly Ln_{II}/n_0 for proton density n_{II} in the old H II region, we obtain a Rayleigh-Taylor unstable time of roughly $(n_{II}/n_0)^{1/2} = (r_{II}/r_0)^{1/4} \approx 0.3$ times τ_D, using the inverse of the layer thickness as the unstable wavenumber (and $N_0 = n_3 = 1$).

Evidently the old CPS layer will be pushed aside and broken apart as soon as the stars emerge from the front of the layer and begin to ionize the ambient cloud. Thus there is no problem in exposing the newly formed stars. The fate of the old CPS layer is uncertain. Of course, more of it will become ionized by the old and new OB subgroups, but it is possible that dense neutral globules will form from its un-ionized fragments, like those observed in the Orion Nebula (Sim 1968; Bok, Cordwell, and Cromwell 1971; Dyson 1973).

A sequence of progressive evolution of CPS layers can actually be identified in such sources as M8, M17, M42, IC 1795, and IC 1805. We may characterize this evolution by four observable stages: (1) the formation of protostars in the CPS layer, which may be represented by maser sources and/or infrared sources (e.g., W3 IRS-5, the Kleinmann-Low region of M42, and M17 SW); (2) the formation of dense ($n \geqslant 10^4$ cm^{-3}) compact H II regions within the CPS layer (e.g., W3, main component); (3) the emergence of stars from the CPS layer and the appearance of a lower density ($n \leqslant 10^3$ cm^{-3}) H II region which expands away from the molecular cloud, and which may obscure the new cluster (e.g., M17 and Herschel 36 in M8), and (4) the final disruption and dissipation of the CPS layer which results in the exposure of a visible cluster (e.g., Trapezium, IC 1805, NGC 6530).

b) A Comparison between the CPS Cluster and Observed OB Subgroups

Several observed properties of OB associations naturally follow from this model. We first review the way in which the derived scales of time, distance, and mass depend on the molecular cloud density and LC luminosity of the shock-driving OB subgroup. Then the influence of a (small) magnetic field is analyzed in order to explain the observed alignment of OB subgroups along the galactic plane, and finally, we suggest several possibilities for the origin of the observed cluster expansion.

i) *Scaling Laws and Observations*

One of the more interesting properties of the derived gravitational instability in the CPS layer is that the time scale for the instability to occur, t_I in the notation of § IV, is very nearly independent of the LC luminosity of the shock-driving OB subgroup, characterized by the dimensionless quantity N_O, which is the number of O stars in a column of area 10 pc^2. This is evident from the similar way in which the CPS layer thickness and the CPS Jeans length scale with the post shock pressure (recall eqs. [A18] and [A20]). The CPS layer thickness varies roughly with time t, in proportion to $tv_s n_0 kT/P$, which is proportional to $n_0^{1/2}Tt/P^{1/2}$ (from eq. [6]) for CPS pressure P, temperature T, and preshock density n_0. The Jeans length of the CPS gas scales with $(T/n)^{1/2}$ for CPS density n, and this is proportional to $T/P^{1/2}$. Thus the CPS layer thickness will equal a constant times the CPS Jeans length (eq. [A21]) at a time which is independent of the CPS temperature and pressure, and which depends only on the preshock density. There will be a multiplicative constant, however, which depends on the power of r in the expression for $v_s(r)$.

It is interesting that the instability time, t_I, happens to be less than the main-sequence lifetime of an OB star for observed molecular cloud densities. If this were not the case, the ionization-shock front would probably disappear due to a lack of LC radiation before a new cluster could form. It is also noteworthy that t_I is slightly larger than the growth time of a Jeans instability in the primordial molecular cloud $(4\pi G\rho_0)^{-1/2}$. This may be a serious problem with the model if the unshocked molecular cloud is actually collapsing at the free-fall rate, but several observations support the idea that such free-fall collapse is not generally occurring for the molecular cloud as a whole (Zuckerman and Evans 1974; Lada 1975; Milman 1975). The fact that star formation occurs over a period of some 10^7 years in individual cloud complexes also argues against uninhibited collapse. This certainly warrants further research. (We return to this problem in § VI.)

The distance scale, r_I, of 10–20 pc is well suited to the observations of OB subgroups (Blaauw 1964). It depends weakly on the LC luminosity of the shock-driving OB subgroup ($\sim N_O^{1/5}$) and scales roughly as $n_0^{-4/5}$ for molecular cloud density n_0. Unfortunately, only a few associations have enough well-defined subgroups to be able to trace the variation of r_I from burst to burst. The Orion association is one good case, however. We see from Figure 4 of Blaauw (1964) that the separation between subgroups has decreased with time, that is, the oldest pair of subgroups (Ori Ic and Id) have the greatest separation, while the youngest pair (Ori Ia and Ib) have the least. This may be the result of either an increase with time of the density of the primordial cloud (due to slow contraction of the original cloud) or a spatial increase in the cloud density in the direction of old to young subgroups.

Another interesting characteristic of this model is the possible rapid convergence of the mass of the subgroups to a constant value. This results from the weak dependence of M_{CPS} on N_O in equation (24). If the stellar luminosity function or mass function is the same for each subgroup, and if the fraction of the CPS gas which froms stars is also constant, then the total LC luminosity of a subgroup, measured here by the variable N_O, should be linearly proportional to the CPS mass, or $N_O = \beta M_{CPS}$ for M_{CPS} in solar masses. The total mass of a new subgroup will then scale with a small power ($\frac{1}{5}$) of the total mass of the previous subgroup from equation (24). The sequence of subgroups will therefore converge after only a few steps to a constant total mass, $M_{CPS,0}$, given by

$$M_{CPS,0} = (3100)^{5/4}\beta^{1/4}n_3^{1/4}\, M_\odot\,. \qquad (27)$$

This agrees with the observed regularity of the stellar populations from subgroup to subgroup (Blaauw 1964), and suggests furthermore that the energy or type of event which initially triggered a particular sequence of OB subgroups cannot easily be ascertained from characteristics of the present association (cf. § VI).

ii) *Magnetic Alignment*

One especially favorable aspect of this method of star formation concerns the magnetic inhibition to gravitational collapse. The magnetic energy per gram will be greater in the molecular cloud than it will be in that part of the compressed CPS layer which propagates nearly parallel to the magnetic field, $\boldsymbol{B}_0$, in the cloud. This is because the gas density increases relative to the magnetic energy density during a compression parallel to the magnetic field. The gravitational energy per gram will be the same for the critically unstable elements, however, if their temperatures are the same, from simple Jeans-length arguments. Thus the magnetic energy density in the unshocked cloud is larger relative to the gravitational energy density of a critically unstable element than it will be in that part of the CPS layer which propagates nearly parallel to $\boldsymbol{B}_0$. This implies that postshock star formation may alleviate some of the usual problems with magnetic inhibition to gravitational collapse.

The opposite will be true for that part of the CPS layer which propagates perpendicular to $\boldsymbol{B}_0$. We estimate here the maximum angle between the direction of propagation of the star-forming part of the CPS layer and the magnetic field in the unshocked molecular cloud.

The angle between the direction of propagation of the shock and the magnetic field in the cloud will be denoted by $\theta_i (0 < \theta_i < \pi/2)$, where the subscript i equals 1 and 2 for preshock and postshock sides, respectively. We assume for simplicity that the magnetic field in the cloud is relatively small so that the gas and kinetic pressures behind the shock dominate the magnetic pressure there. This is not essential to the argument, but it is compatible with our lack of consideration for magnetic field in the rest of this analysis. Then the component of $\boldsymbol{B}_0$ which is perpendicular to $\boldsymbol{v}_s$ will increase in strength in proportion to the compressed gas density in order to preserve magnetic flux. The component of $\boldsymbol{B}_0$ parallel to $\boldsymbol{v}_s$ remains unchanged. Then if ϵ denotes the ratio of the CPS density to the unshocked cloud density,

$$\epsilon = \frac{\tan \theta_2}{\tan \theta_1}\,, \tag{28}$$

and the total magnetic field strengths on each side of the shock have the ratio

$$\frac{B_2}{B_1} = \frac{\cos \theta_1}{\cos \theta_2} \approx (1 + \epsilon^2 \tan^2 \theta_1)^{1/2}\,, \tag{29}$$

where the approximation is valid for the small angles θ_1 that we shall be considering (i.e., $\cos \theta_1 \approx 1$).

Simple virial-theorem arguments may be used to show that the minimum mass, M_c, for gravitational instability in a magnetic field varies as the cube of the field strength, B, and as the inverse square of the gas density (Mestel 1971). Thus the ratio of the critical mass for collapse in the CPS layer to that in the molecular cloud ahead of the shock is

$$\frac{M_{c2}}{M_{c1}} = \frac{(1 + \epsilon^2 \tan^2 \theta_1)^{3/2}}{\epsilon^2}\,. \tag{30}$$

Since $\epsilon \approx 100 N_{\mathrm{O}}^{2/5} n_3^{-3/5} T_2^{-1}$ from equation (20), we have that

$$\tan \theta_1 \approx \left(\frac{M_{c2}}{\epsilon M_{c1}}\right)^{1/3}$$
$$\approx 0.22 N_{\mathrm{O}}^{-2/15} n_3^{1/5} T_2^{1/3} \left(\frac{M_{c2}}{M_{c1}}\right)^{1/3}\,. \tag{31}$$

If the magnetic field in the molecular cloud is indeed significant, then generally $M_{c2} < M_{c1}$; that is, smaller masses will be unstable in the CPS layer than in the undisturbed cloud and, for $N_{\mathrm{O}} \approx n_3 \approx 1$,

$$\theta_1 < 12°\,. \tag{32}$$

Evidently the sequence of OB stars will naturally follow the gross alignment of the magnetic field in the primordial cloud and will therefore tend to lie along the galactic plane, as observed.

iii) *Cluster Expansion*

One other aspect of OB subgroups is their physical expansion, which is often difficult to separate from an apparent (but artificial) expansion due to the relative motion between the cluster and the observer. Nevertheless, physical expansion velocities have been extracted for several OB associations, the most notable being II Per (Blaauw 1964), where OB stars have an average space velocity of 9 km s^{-1} relative to the centroid, not including the runaway star ξ Per. Another cluster near o Per is expanding with a velocity of only 2 km s^{-1} (Frederick 1956; Blaauw 1964), so the total cluster energies may vary by quite a bit in the same association.

Several attempts have previously been made to explain this expansion, some of which involve the motion of shock fronts (Oort 1954; Öpik 1953). It is almost certain (Spitzer 1968*a*) that a cluster which forms by the collapse and fragmentation of a single, bound cloud will not become completely unbound after the stars turn on, as proposed by Zwicky (1953) and McCrea (1955). This would require the ionization and disruption of a large fraction of the cloud's mass in only a few million years; in addition, the observed stellar velocities would have had to be present before the disruption of the cloud (Oort 1954), requiring unreasonably large densities. Star formation in shock fronts seems to be a better way to form expanding associations.

Unfortunately, the present one-dimensional analysis with a homogeneous molecular cloud cannot account for any relative velocity between the protostars. Actual shock fronts may diverge somewhat, although stars will tend to form within the angular limits set by the magnetic field (see above). Furthermore, cloud inhomogeneities will cause different parts of the shock to evolve separately with different velocities, so the resulting protostars will have an average relative velocity which is proportional to the fluctuations in the molecular cloud density: $|\Delta v_s|/v_s = \Delta n_0/2n_0$, from equation (6). Large-scale turbulence in the primordial molecular cloud will similarly introduce a spread in protostellar velocities, since v_s is measured relative to the gas immediately ahead of the shock. The nonzero extent of the shock-driving OB subgroup, parallel to the direction of propagation of the shock, may also cause a spread in shock velocities since different parts of the shock will be at different distances from the nearest star. Then $|\Delta v_s|/v_s \sim \Delta r/4r$. These and other possible contributions to the relative fluctuation of the protostellar velocities may or may not add up to be significant. The dynamical relaxation of the CPS protocluster may also introduce some dispersion, but the process of star-ejection during dynamical relaxation is not likely to account for the expansion of the cluster as a whole unless a tightly bound core of stars (i.e., a subcluster) remains to absorb the energy of the ejected stars (Lynden-Bell 1967; Gott 1973). In any case, it is evident that postshock formation of stars may more readily lead to expanding clusters than will the simple collapse and fragmentation of a large cloud. However, the exact nature of the expansion may depend on inhomogeneities in the clouds and in the shock-driving clusters or upon the spherical expansion of the shock, which are not considered in the present paper.

VI. STAR FORMATION IN THE GALAXY

The agreement between the proposed mechanism of postshock star formation and the observations of

OB associations should not be interpreted as an indication that all stars may be formed in this manner. On the contrary, observations of stars with relatively low mass ($M \lesssim 9\ M_\odot$) and late spectral type (roughly B3 or later), such as T Tauri stars, seem to require other formation mechanisms. As pointed out by Herbig (1962, 1970), the proximity of T Tauri stars to the Taurus dark clouds strongly suggests that the formation of these stars took place without the aid of H II regions and I fronts, since there is no observational evidence for the presence of massive stars in these regions. Recent observations of molecular clouds which are not associated with detectable H II regions or massive stars also indicate that T Tauri stars can form without the aid of massive stars or I fronts (e.g., Loren, Vanden Bout, and Davis 1973; Lada *et al.* 1974; Loren 1976).

Perhaps it is in connection with the formation of these later-type stars that the Hoyle (1953) picture of gravitational collapse and fragmentation is important. There is some observational evidence for this since T Tauri stars and H-H objects are often associated with high-density fragments in molecular clouds (Lada *et al.* 1974; Strom, Strom, and Grasdalen 1975); these fragments appear to be very similar in size (1–2 pc) and density (10^4 cm^{-3}) from cloud to cloud. Examples are found in Mon R2 (Kutner and Tucker 1975), ρ Oph (Encrenaz 1974; Gottlieb *et al.* 1977), and near NGC 1333, M78 (Lada *et al.* 1974), NGC 2071 (Gottlieb *et al.* 1977; Strom *et al.* 1975*a*), and CrA (Strom *et al.* 1975*b*; Loren, Peters, and Vanden Bout 1974). Since the recent theoretical studies of cloud fragmentation by Gaustad (1963), Lynden-Bell (1973), and Silk (1976) generally derive small protostellar masses, it may be that the smaller-mass T Tauri stars are formed as a result of undisturbed cloud fragmentation and that the more massive OB stars tend to form in high-density shocked gas. The reason for this difference is unknown, but it may be related to the high temperatures and densities which are likely to occur in the CPS gas at the onset of instability, as mentioned in § IV*b*(ii).

Unfortunately, observations may not provide a clear distinction between star formation which occurs in large cloud fragments and in CPS layers. This results from a strong observational selection effect which may be derived from the results of § IV. Recall from equation (18) that the delay time, t_I, for gravitational instability to occur in the CPS layer scales as $n_0^{-1/2}$ for molecular cloud density n_0. This means that a shock which propagates into a cloud composed of high-density fragments and a lower-density interfragment gas will first cause stars to form in that part of the CPS layer which penetrates the fragments. Thus OB stars as well as T Tauri stars may correlate spacially with cloud fragments. In M17, for example, the present site of OB star formation is at the *edge* of a cloud fragment (see Fig. 1) as expected from the present theory. The perspective is not as favorable in Orion, however, and the observed region of high molecular density at the edge of the nebula may be either a cloud fragment, part of a CPS layer, or both.

There is, however, a strong observational *advantage* to having different mechanisms for different mass ranges, and this concerns the exposure of the newly formed stars. If the unshocked part of the molecular cloud forms low-mass stars by internal fragmentation, then these stars must eventually be brought into view. For a large, optically thick molecular cloud, this exposure must be related to the dissipation of the cloud. Thus we return to I-S fronts as a means of cloud disruption: in addition to their direct role in star formation, ionization-driven shocks may also play an indirect role in the creation of visible star clusters by clearing away the molecular cloud which surrounds the cluster. Observations may support this idea. OB associations have long been known to contain T associations within their boundaries. Unfortunately, not enough is known about T Tauri stars to properly determine their place in the evolution of an OB association; members of a given T association may span a wide range of ages (10^5–10^7 yr; Strom *et al.* 1975*a*), so it is not even clear if T Tauri stars formed at the same time as the OB stars. Since molecular clouds seem to form T Tauri stars whether or not H II regions are present, it is possible that many T Tauri stars will form in a molecular cloud before the onset of OB star formation. If OB stars never form, then large populations of T Tauri stars will remain embedded in the clouds, and will be obscured from view for long periods of time ($\sim 10^8$ yr; see Strom *et al.* 1975b). However, with the onset of sequential OB subgroup formation, I fronts and shock fronts will clear and dissipate cloud material from the neighborhood of existing stars. The presence of visible T associations within OB associations may thus be a consequence of effective cloud dissipation by the ionization-shock front system. It is not necessary, from an observational point of view, that T Tauri stars be formed in the CPS layer along with the more massive OB stars, but it is necessary that they become exposed.

Finally we note that the requirement that this sequential formation model must be initiated means that massive stars may also be formed by other mechanisms. Supernova shocks, cloud-cloud collisions density-wave shocks, or even normal cloud collapse may provide alternative mechanisms for OB star formation. In the case of supernovae, there has been only one observation where a supernova may have initiated some type of star formation. This is the Origem Loop, studied by Berkhuijsen (1974). The problem with the detection of correlations between supernova remnants and young stars is that the remnants are generally short lived compared to the free-fall or turn-on time of protostars. The Origem Loop was reported to be 10^6 years old, however, and the associated young stars were given half that age. This is probably older than any other known supernova remnant (see however, Berkhuijsen 1971), so it may be an exceptionally favorable case for the observation of this effect.

The possibility that stars can form during the collision between two molecular clouds may be illustrated by the case of NGC 1333 (Loren 1976). The observed stars are not massive OB stars, and the cloud-cloud collision frequency is generally believed to be low (i.e., $<10^{-7}\,\mathrm{yr}^{-1}$; see Spitzer 1968*b*), suggesting that this may not be an important means of initiating the sequence of OB subgroups. The environment of a spiral density wave may modify the collision rate, however, so this possibility should not be immediately ruled out. Clouds which stream past a spiral density wave and into the shocked intercloud medium may experience a ram pressure which tends to oppose their tangential motion in the galactic disk (Mouschovias, Shu, and Woodward 1974). They may thus collide with other clouds which have already slowed down, or they may simply become shocked at their leading edges as in the calculations by Woodward (1975). The formation or growth of clouds in a spiral density wave may lead quite naturally to protostellar collapse (Mouschovias, Shu, and Woodward 1974) so that a complete theory of star formation or, in particular, of the initiation of a sequence of OB subgroups, may be possible only after the process of cloud formation is understood.

One interesting possibility is that the molecular cloud may grow continuously at one end by the accretion of interstellar gas, and may dissipate continuously at the other end with star-forming I-S fronts. The accumulation of new cloud material at the one end may be the result of the funneling of lower-density interstellar material by a process associated with the spiral density wave. Several calculations (Field and Saslaw 1965; Mouschovias, Shu, and Woodward 1974) show that clouds may be formed in a related manner, and observations of other spiral galaxies show the alignment of dark clouds and OB associations along the spiral structure (and perpendicular to it) in a manner which supports this directivity (e.g., Lynds 1970). There is no obvious reason why there should be a steady state, but an estimate for the average emergent particle flux at the dispersing end of the cloud, $n_0 r_\mathrm{I}/t_\mathrm{I} \approx 5 \times 10^8 N_0{}^{1/5} n_3{}^{7/10}$ hydrogen atoms $\mathrm{cm}^{-2}\,\mathrm{s}^{-1}$ from equations (16) and (18) compares favorably with an influx of unit density material (i.e., a mix of diffuse clouds and intercloud material) at a velocity of, say, $10\,\mathrm{km\,s}^{-1}$ (roughly one-third of the component of the velocity of a local spiral density wave which is perpendicular to the spiral) through a funnel which compresses one square scale height (i.e., $150^2\mathrm{pc}^2$) to the cross-sectional area of a typical molecular cloud ($50\,\mathrm{pc}^2$). This may not be more than a numerical coincidence, but it emphasizes the need to understand cloud formation along with star formation.

VII. CONCLUSIONS

The formation of massive stars in OB associations seems to occur in a sequential manner, in the sense that star formation moves along the galactic plane from what was presumably one edge of a primordial cloud to its center or the other edge of the cloud. The evidence for such a progression is available from observations of the associations themselves, but it is also apparent from detailed maps of molecular clouds, I-S fronts, IR sources, and masers. We have shown that such a sequence may occur quite naturally as an I-S front moves through the cloud: the material that accumulates between the I and S fronts becomes unstable to gravitational collapse when it reaches a threshold column density. The new stars that form in the compressed layer migrate toward the front of the layer as the shock slows down. Within about one-half million years, their high-pressure H II regions can break up the remains of the cool shocked gas from which they formed and initiate a new I-S front and, therefore, a new generation of stars. The observed similarity of OB subgroup populations, subgroup expansion, and the alignment of the association along the galactic plane are also natural consequences of such a theory.

Several important differences appear between the usual picture of spherical collapse and fragmentation of a primordial cloud and the plane-parallel compression of the same cloud (into a cooled postshock layer). One is that the magnetic inhibition to gravitational collapse is not as severe in the latter case if the shock compression is roughly parallel to the magnetic field in the cloud. Furthermore, the temperature of CPS gas will be higher than that in a fragmenting cloud because warm grains in the nearby H II region and the OB stars themselves can heat the grains in the CPS layer. Since the unstable masses depend sensitively on the temperatures, this CPS layer may eventually form larger protostars than will a cooler, remote part of the same cloud. Thus we believe that the proposed mechanism is ideal for the creation of massive stars, in addition to providing an explanation for the observed physical structure of OB associations.

Finally it must be emphasized that any theory of star formation will be incomplete without a corresponding theory of cloud formation. Galactic spiral structure not only delineates regions of intense star formation, but also delineates systems of dense clouds. The results of the present paper suggest that a dense molecular cloud ($n_0 \approx 10^3\,\mathrm{cm}^{-3}$) will be somewhat volatile to star formation; and, once triggered, it will virtually self-destruct as OB subgroups generate other OB subgroups until the cloud is exhausted. The most fundamental observational problem may eventually be in the detection of the early stages of cloud formation. Apparently, this must be approached with a firm understanding of spiral density waves, and of their influence on dense molecular clouds.

We are grateful to Drs. G. B. Field, W. G. Mathews, and L. L. Cowie for useful comments. One of us (B. G. E.) acknowledges support by a Junior Fellowship from the Society of Fellows at Harvard University.

APPENDIX

THE STABILITY OF AN ISOTHERMAL, PLANE-PARALLEL MEDIUM WITH AN EXTERNAL PRESSURE

A very thin, plane-parallel layer of self-gravitating gas will be unstable to collapse in a transverse direction (i.e., parallel to the plane) for any value of the midplane density as shown by Ledoux (1951) and Simon (1965). The present problem is slightly different from that considered by these authors, because in this case there is an external pressure which acts on each side of the finite layer. Unlike the situation with no external pressure, a pressurized layer will not be unstable to transverse perturbations for any value of the density at midplane. It will be unstable only for sufficiently large accumulations of gas, where the internal density is greater than some critical value.

We determine here the distribution of pressure and density inside an isothermal, plane-parallel layer (the CPS layer) which is subject to known pressures P_1 and P_2 on the two planar boundaries. The pressure on one boundary, P_1, will be the pressure at the I front, $\xi P_{\rm II}$ in the notation of § IV*a*, while the pressure at the other boundary, P_2, will be the pressure at the S front, and it will be greater than P_1 if the shock decelerates. In general, we write

$$P_2 = \gamma P_1 , \tag{A1}$$

where $\gamma = 4/3$ in the present case.

We choose a coordinate system which is comoving with the CPS layer. Then the deceleration of this layer in an inertial coordinate system, denoted here by g (but equal to $-\dot{v}_s$ in the notation of § IV*a*), will enter the equations for the hydrostatic equilibrium of the layer as an effective gravity. If σ is the mass column density in the CPS layer, then this deceleration is related to the pressure difference between the two planar boundaries by the equation

$$g = \frac{P_2 - P_1}{\sigma} = (\gamma - 1)\frac{P_1}{\sigma} . \tag{A2}$$

This follows from Newton's force law and is implicit in the derivation of v_s in § IV*a*.

The density distribution of the self-gravitating layer may then be determined in the usual way (Spitzer 1942) from the hydrostatic force equation, Poisson's equation, and the isothermal equation of state:

$$\nabla P = -\rho\nabla\phi - g\rho , \qquad \nabla^2\phi = 4\pi G\rho , \qquad P = c^2\rho . \tag{A3}$$

The solution is

$$\rho(z) = \rho(0)\cosh^{-2}\left(\frac{z}{H}\right) \equiv \rho(0)(1 - w^2) \tag{A4a}$$

$$\nabla\phi(z) = 4\pi G\rho(0)H\tanh\left(\frac{z}{H}\right) - g \tag{A4b}$$

where

$$H = \frac{c}{[2\pi G\rho(0)]^{1/2}} . \tag{A5}$$

The internal pressure follows the same hyperbolic secant behavior with z from equation (A3c), so the boundary conditions define the extent of the layer above and below the plane $z = 0$. If $P = P_1$ for $z = z_1$ and $P = P_2 = \gamma P_1$ for $z = -z_2$, then

$$\operatorname{sech}^2\left(\frac{z_1}{H}\right) \equiv 1 - w_1^2 = \frac{P_1}{\rho(0)c^2} , \tag{A7a}$$

$$\operatorname{sech}^2\left(\frac{z_2}{H}\right) \equiv 1 - w_2^2 = \frac{\gamma P_1}{\rho(0)c^2} . \tag{A7b}$$

We determine $\rho(0)$ from the requirement that the total mass in a column of unit area, σ, be equal to the integral of $\rho(z)$ over z from $-z_2$ to z_1, i.e., $\sigma = \rho(0)H(w_1 + w_2)$, so that

$$\rho(0)c^2 = \tfrac{1}{2}\pi G\sigma^2 + \frac{(\gamma - 1)^2 P_1^2}{8\pi G\sigma^2} + \frac{(\gamma + 1)P_1}{2} . \tag{A8}$$

Thus the thickness of the layer $(z_1 + z_2)$ and the values of w_1 and w_2, for use in what follows, may be determined from the external pressure P_1 and γP_1 and from the total accumulated mass column density σ using equations (A7) and (A8).

We note that for *large* σ, the layer will have the maximum density $\rho(0)$ in its interior, as opposed to having a (relative) maximum density at the leading face as in equation (12). For large σ, the density distribution in a decelerating layer which extends from z_1 to $-z_2$ (given by eqs. [A4]) is the same as the density distribution in the same part of a layer at rest, which is symmetric about $z = 0$ and which extends all the way from z_1 to $-z_1$. The additional layer from $-z_2$ to $-z_1$ in the second case gravitationally accelerates the rest of the layer (from z_1 to $-z_2$) by exactly the amount g, used as an effective gravity in equations (A3). For *small* σ (as in § IV*a*) the density distribution given by equation (A4a) should approach that in equation (12) where self-gravitation was not included. In this case, the physical layer extends from $+z_2$ (rather than $-z_2$) to $+z_1$, and it experiences a deceleration g which is exactly equal to that produced by the part of a layer at rest, symmetric around $z = 0$, which extends from $+z_2$ to $-z_1$. Thus $\rho(0)c^2 \cosh^{-2}(z/H)$ goes to $P_1 \exp[-g(z - z_2)/c^2]$ as σ goes to zero, as required by the Boltzmann distribution in equation (12).

We now investigate the marginal stability of the CPS layer in the manner outlined by Spitzer (1968*b*). That is, we apply to equations (A3) an infinitestimal perturbation of the density in two dimensions, $\delta\rho(w, x)$, around the equilibrium value $\rho(w)$ in equation (A4a), and we determine the critical wavenumber k_c which satisfies

$$\delta\rho(w, x) = \rho(w) \exp(ik_c x)\theta(w) . \tag{A9}$$

A general solution for $\theta(w)$ in terms of the quantity

$$\nu = k_c H \tag{A10}$$

has been given by Spitzer (1968*b*), but we impose different boundary conditions which are more appropriate for this problem, namely,

$$\theta(w_1) = 0 , \quad \theta(-w_2) = 0 . \tag{A11}$$

These conditions reflect the fact that the pressures on the perturbed outer surfaces are always equal to the unperturbed values P_1 and γP_1, respectively. If $\nu = 1$, these two boundary conditions degenerate to a single equation which requires that $w_1 = 1$ and that the layer be infinite in extent. For $\nu < 1$, we may use equation (A7) and (A11) to determine ν as a function of w_1 or w_2, which are known from P_1 and σ, as shown above. Thus

$$w_2 = (\gamma w_1^2 - \gamma + 1)^{1/2} \tag{A12}$$

and

$$\nu^2 + \nu(w_1 + w_2)\frac{B^\nu + 1}{B^\nu - 1} + w_1 w_2 = 0 , \tag{A13}$$

where

$$B = \left(\frac{1 - w_1}{1 + w_1}\right)\left(\frac{1 - w_2}{1 + w_2}\right) . \tag{A14}$$

Not all values of the pair (w_1, w_2) which satisfy equation (A12) result in a positive (and therefore physically realistic) value of ν, however. The limiting form of equation (A13) as $\nu \to 0$ is

$$\frac{w_1 w_2}{w_1 + w_2} = \frac{-2}{\ln B} , \tag{A15}$$

which may be solved using equations (A12) and (A14) to give the minimum values of w_1 and w_2, denoted by w_{1m} and $w_2 m$, respectively. For $\gamma = 4/3$ (eq. [A1]) we have

$$w_{1m} = 0.85878 , \tag{A16a}$$

$$w_{2m} = 0.80622 . \tag{A16b}$$

The corresponding lower limit to σ, denoted by σ_m, is $\rho_0 H(w_{1m} + w_{2m})$; or for $\gamma = 4/3$ and using equation (A8),

$$\sigma_m = 2.298(P_1/\pi G)^{1/2} . \tag{A17}$$

We conclude that the CPS layer will become gravitationally unstable to transverse perturbations when its mass column density σ and external pressures, P_1 and $\frac{4}{3}P_1$, satisfy equation (A17).

It is illustrative to write the instability criterion in equation (A17) as a comparison between two lengths. One is an effective thickness of the plane parallel layer, L_e, defined here as the ratio of the mass column density of the layer, σ, to an effective mass density given by

$$\bar{\rho} = \mu \frac{P_1}{kT} \tag{A18}$$

for mean molecular weight μ and temperature T. Thus,

$$L_e = \sigma/\bar{\rho}\,. \tag{A19}$$

The second length is the Jeans length of a uniform, infinitely extended gas at the same mass density and mean molecular weight (Spitzer 1968*b*):

$$L_J = \left(\frac{\pi k T}{4G\bar{\rho}\mu}\right)^{1/2}. \tag{A20}$$

It follows from equation (A17) that when

$$L_e \geq 1.46 L_J\,, \tag{A21}$$

the layer becomes gravitationally unstable to large transverse perturbations. The true thickness L of the layer is $z_1 + z_2$, or

$$L = 2.4H = \frac{2.0c^2}{\pi G \sigma_m} = 0.38 L_e \quad (\sigma = \sigma_m) \tag{A22}$$

at the onset of gravitational instability, from equations (A5), (A7), (A8), (A17), (A18), and (A19).

The fact that there is any stability at all for a self-gravitating stratified layer with an external pressure is an interesting result since Ledoux (1951) obtained a finite unstable length for any value of the midplane density when there was no external pressure. The stability found here corresponds to the physical fact that the rms velocity at the midplane is increased by an external pressure, so it can be larger than the ratio of an unstable length to the free-fall time of that perturbation. Such perturbations will simply propagate as waves, and there will be no instability. This is possible for a plane-parallel layer because the free-fall time increases without limit as the extent of the perturbation parallel to the plane becomes infinite (see Simon 1965). Thus the average velocity of the freely falling material (equal to the perturbation length divided by this free-fall time) approaches a constant for infinite perturbations, and it can be less than the rms velocity if the total mass in the layer is small. It is evident from equations (A7)–(A14) that the pressureless case ($P_1 = 0$) is a singularity of equation (A15) where B becomes zero and ν becomes equal to w_1, which equals w_2 and 1. Thus only an (infinitesimally) small external pressure is necessary to give the observed stability (as manifested by a fixed lower limit to w_1 which is independent of P_1) for (infinitesimally) small values of σ satisfying $\sigma < \sigma_m$.

For the sake of completeness, we also give the stability criterion in the case where $\gamma = 1$, that is, where the pressures on each side of the layer are the same ($P_1 = P_2$). A similar analysis shows that

$$\sigma_m = 2.135(P_1/\pi G)^{1/2} \quad (\gamma = 1)\,. \tag{A23}$$

The coefficient in equation (A21) then changes from 1.46 to 1.36.

REFERENCES

Aannestad, P. A. 1973, *Ap. J. Suppl.*, **25**, 205.
Ambartsumian, V. A. 1955, *Observatory*, **75**, 72.
Balick, B., Gammon, R. H., and Hjellming, R. M. 1974, *Pub. A.S.P.*, **86**, 616.
Becklin, E. E., Beckwith, S., Gatley, I., Matthews, K., Neugebauer, G., Sarazin, C. and Werner, M. W. 1976, *Ap. J.*, **207**, 770.
Beetz, M., Elsässer, H., Poulakos, C., and Weinberger, R. 1976, preprint.
Berkhuijsen, E. M. 1971, *Astr. Ap.*, **14**, 252.
———. 1974, *Astr. Ap.*, **35**, 429.
Blaauw, A. 1962, in *Interstellar Matter in Galaxies*, ed. L. Woltjer (New York: Benjamin), p. 32.
———. 1964, *Ann. Rev. Astr. Ap.*, **2**, 213.
Bok, B. J., Cordwell, C. S., and Cromwell, R. H. 1971, in *Dark Nebulae, Globules and Protostars*, ed. B. T. Lynds (Tucson: University of Arizona Press), p. 57.
Churchwell, E., and Felli, M. 1970, *Astr. Ap.*, **4**, 309.
Cruz-Gonzales, C., Recillas-Cruz, E., Castero, R., Peimbert, M., and Torres-Peimbert, S. 1974, *Rev. Mexicana Astr. Ap.*, **1**, 211.
Dyson, J. E. 1973, *Astr. Ap.*, **27**, 459.
Elliot, K. H., and Meaburn, J. 1974, *Astr. Ap.*, **34**, 471.
Elmegreen, B. G., and Lada, C. J. 1976, *A.J.*, **81**, 1089.
Elmergreen, B. G. 1976, *Ap. J.*, **205**, 405.
Encrenaz, P. J. 1974, *Ap. J. (Letters)*, **189**, L135.
Field, G. B., and Saslaw, W. C. 1965, *Ap. J.*, **142**, 568.
Frederick, L. W. 1956, *A.J.*, **61**, 437.
Gaustad, J. E. 1963, *Ap. J.*, **138**, 1050.
Gott, J. R. 1973, *Ap. J.*, **186**, 481.
Gottlieb, C. A., Ball, J. A., Litvak, M. M., and Lada, C. J., 1977, in preparation.
Gottlieb, C. A., Lada, C. J., Gottlieb, E. W., Lilley, A. E., and Litvak, M. M. 1975, *Ap. J.*, **202**, 655.
Gull, S. F., and Martin, A. H. M. 1975, in H II *Regions and Related Topics*, ed. T. L. Wilson and D. Downes (New York: Springer-Verlag), p. 369.
Habing, H. J., Israel, F. P., and de Jong, T. 1972, *Astr. Ap.*, **17**, 329.
Harris, S., and Wynn-Williams, C. G. 1976, *M.N.R.A.S.*, **174**, 649.
Herbig, G. H. 1960, *Ap. J. Suppl.*, **4**, 337.
———. 1962, *Adv. Astr. Ap.*, **1**, 47.
———. 1970, *Liège Symposium*, **19**, 13.
Hoyle, F. 1953, *Ap. J.*, **118**, 513.
Israel, F. P. 1976, *Astr. Ap.*, **48**, 193.
Kahn, F. D. 1954, *B.A.N.*, **12**, 187.
Kutner, M. L., Thaddeus, P., Tucker, K. D., and Chin, G. 1977, *Ap. J.* (in press).
Kutner, M. L., and Tucker, K. D. 1975, *Ap. J.*, **199**, 79.
Lada, C. J. 1975, Ph.D. dissertation, Harvard University.
Lada, C. J., and Chaisson, E. J. 1975, *Ap. J.*, **195**, 367.
Lada, C. J., Dickinson, D. F., Gottlieb, C. A., and Wright, E. L. 1976*a*, *Ap. J.*, **207**, 113.

Lada, C. J., Gottlieb, C. A., Litvak, M. M., and Lilley, A. E. 1974, *Ap. J.*, **194**, 609.
Lada, C. J., Gull, T. R., Gottlieb, C. A., and Gottlieb, E. W. 1976*b*, *Ap. J.*, **203**, 159.
Lasker, B. M. 1967, *Ap. J.*, **149**, 23.
Ledoux, P. 1951, *Ann d'Ap.*, **14**, 438.
Loren, R. B. 1976, *Ap. J.*, **209**, 466.
Loren, R. B., Peters, L. L., and Vanden Bout, P. A. 1974, *Ap. J.* (*Letters*), **194**, L103.
Loren, R. B., Vanden Bout, P. A., and Davis, J. H. 1973, *Ap. J.* (*Letters*), **185**, L67.
Lynden-Bell, D. 1967, *M.N.R.A.S.*, **136**, 101.
———. 1973, in *Dynamical Structure and Evolution of Stellar Systems*, ed. G. Contopoulos, M. Hénon and D. Lynden-Bell (Geneva: Geneva Observatory).
Lynds, B. T. 1970, in *IAU Symposium 38, The Spiral Structure of Our Galaxy*, ed. W. Becker and G. Contopoulos (New York and Dordrecht: Reidel), p. 26.
McConnell, D. J. 1968, *Ap. J. Suppl.*, No. 147, **16**, 275.
McCrea, W. H. 1955, *Observatory*, **75**, 206.
Meaburn, J. 1975, *Ap. Space Sci.*, **35**, L5.
Mendis, D. A. 1968, *M.N.R.A.S.*, **140**, 435.
Mestel, L. 1971, *Quart. J.R.A.S.*, **12**, 402.
Mezger, P. G., and Wink, J. E. 1975, in H II *Regions and Related Topics*, ed. T. L. Wilson and D. Downes (New York: Springer-Verlag), p. 408.
Milman, A. S. 1975, *Ap. J.*, **202**, 673.
Mouschovias, T. Ch., Shu, F. U., and Woodward, P. R. 1974, *Astr. Ap.*, **33**, 73.
Oort, J. H. 1954, *B.A.N.*, **12**, 177.
Oort, J. H., and Spitzer, L., Jr. 1955, *Ap. J.*, **121**, 6.
Öpik, E. J. 1953, *Irish A.J.*, **2**, 219.
Pottasch, S. 1958, *B.A.N.*, **14**, 29.
Sajn, G. A. 1954, *Astr. Zh.*, **31**, 217.
Silk, J. 1977, *Ap. J.*, **214**, 718.
Sim, M. E. 1968, *Pub. Roy. Obs. Edinburgh*, **6**, 8.
Simon, R. 1965, *Ann d'Ap.*, **28**, 40.
Spitzer, L., Jr. 1942, *Ap. J.*, **95**, 329.
———. 1968*a*, in *Nebulae and Interstellar Matter*, eds. B. M. Middlehurst and L. H. Aller (Chicago: University of Chicago Press), p. 1.
———. 1968*b*, *Diffuse Matter in Space* (New York: Interscience).
Strom, K. M., Strom, S. E., Carrasco, L., and Vrba, F. J. 1975*a*, *Ap. J.*, **196**, 489.
Strom, S. E., Strom, K. M., and Grasdalen, G. L. 1975*b*, *Ann. Rev. Astr. Ap.*, **13**, 187.
Woodward, P. R. 1975, *Bull. AAS*, **7**, 258.
Wynn-Williams, C. G. 1971, *M.N.R.A.S.*, **151**, 397.
Zuckerman, B. 1973, *Ap. J.*, **183**, 866.
Zuckerman, B., and Evans, N. J. 1974, *Ap. J.* (*Letters*), **192**, L149.
Zwicky, F. 1953, *Pub. A.S.P.*, **65**, 205.

Bruce G. Elmegreen and Charles J. Lada: Center for Astrophysics, 60 Garden Street, Cambridge, MA 02138